

Detection and Mitigation of Static Multipath in L1 Carrier Phase Measurements Using a Dual-Antenna Approach

M.C. Santos

Department of Geodesy and Geomatics Engineering,
University of New Brunswick, P.O. Box 4400, Fredericton, New Brunswick, Canada, E3B 5A3

J.C.F. Farret

Departamento de Engenharia Rural, Universidade Federal de Santa Maria, Santa Maria, Brazil

Abstract. Multipath remains a major error source in both static and kinematic positioning. For example, it takes a toll in the carrier phase, causing the receiver to measure a distorted phase. Various improvements in receiver and antenna technologies, as well as modelling strategies, have resulted in better ways of coping with this error source. Multipath has been shown to be highly correlated for an array of closely spaced antennas. This fact has allowed various investigations using different antenna/receiver array configurations. In our investigation, we have used a configuration based on two closely spaced antennas linked to a single GPS receiver. Our methodology introduces a temporal factor in the measurements, with the assumption that multipath parameters and satellite geometry have a slow variation in time and space. This paper presents a spectral analysis, which intends to evaluate the performance of the multipath parameters estimation process. The analysis compares estimated multipath signal with the original input data that feeds the estimation process.

Keywords. Global Positioning System, multipath, spectral analysis.

1 Introduction

Multipath can be defined as a phenomenon in which an electromagnetic signal arrives at the receiver site following two or more different paths [Wells et al., 1986]. GPS receivers track a composite signal made up of direct and reflected components. Errors in both pseudorange and carrier phase measurements can occur as a consequence of multipath, depending mostly on the geometry of the reflecting objects, the antenna, and the satellites.

Multipath has been treated in many different ways. The first and most practical way is to avoid it

by means of an appropriate site selection. Others rely on improvements to antenna and receiver hardware design. Modelling of multipath is another alternative. Several examples are found in the literature, such as the one using carrier phase smoothing techniques [Hatch, 1982], spectral analysis and signal repeatability [Axelrad et al., 1994], analysis of signal-to-noise ratio [Reichert and Axelrad, 1999; Kim and Langley, 1999] multiple reference stations [Raquet and Lachapelle, 1996], and multiple antennas [Ray et al., 1999].

In our research we used a configuration of two closely spaced antennas (forming an 11-cm long baseline) connected to the same receiver. Therefore, data from the two antennas were simultaneously registered. The methodology, along with initial results, has been described in Farret and Santos [2000] and is summarized in section 2. Results have indicated that the efficiency of the method can generally reach up to 65%. By efficiency we mean the ratio between the estimated multipath vis-à-vis the measured one.

In this paper we have investigated how well the multipath parameter estimation process takes place. This investigation has been accomplished by comparing the spectra of residual single difference signal (composed of multipath plus noise) with the spectra of a signal computed from the estimated multipath parameters.

2 Methodology

A methodology has been formulated aimed at mitigation of static multipath affecting a reference station. This methodology has been built based on two basic assumptions. First, that signals collected by close-by antennas are highly correlated. Second, that the multipath characteristics will not vary over a very short period of time.

A theoretical representation of the differential error due to multipath (between two antennas), $\Delta\Psi_0$ minus $\Delta\Psi_1$, is given by the following equation, where subscript 0 refers to the reference antenna and subscript 1 to the close-by antenna:

$$\Delta\Psi_0 - \Delta\Psi_1 = \arctan \left\{ \frac{\alpha_0 \sin \gamma_0 - \alpha_0 \sin \gamma_1}{1 + \alpha_0 \cos \gamma_0 - \alpha_0 \cos \gamma_1} + \frac{\alpha_0^2 \sin(\gamma_0 - \gamma_1)}{\alpha_0^2 \cos(\gamma_0 - \gamma_1)} \right\}. \quad (1)$$

The symbol α_0 represents the modified reflection coefficient (assumed to be the same for both antennas due to their proximity) and γ_0 the reflected signal phase at the reference station. The term γ_1 for antenna 1 and can be given as (e.g., Ray et al. [1999]):

$$\gamma_1 = \gamma_0 + \frac{2\pi s_{01} \cos(A_0 - \beta_{01}) \cos \nu_0}{\lambda}, \quad (2)$$

where s_{01} is the distance between antennas 0 and 1, A_0 is the azimuth of reflected signal, β_{01} is the azimuth of the vector formed by the phase centres of both antennas and ν_0 is the elevation of the reflected signal.

Equations (1) and (2) are combined to form the system of equations used in an Extended Kalman Filter (EKF). The choice of an EKF is because of the non-linearity of the system of second order partial differential equations of the involved expressions, to the low knowledge of the temporal variation of the parameters and to the high accuracy of the measurement system. For the system modelling a Gauss-Markov process is used. The estimated multipath parameters are: α_0 , γ_0 , A_0 and ν_0 .

Data (in this case, L1 carrier phase observations) collected by two closely spaced antennas connected to the same receiver are used to form a single difference (SD) observable time series. As many errors as possible are eliminated or modelled from this time series on such a short baseline (in our experiment, of 11 cm). The satellite clock, and the ionospheric and the tropospheric terms are already eliminated during the process of single differencing. The receiver clock term is eliminated because both antennas are linked to the same receiver and it is the same for both antennas. The geometric term can be calculated from the known antenna and satellite coordinates and then removed for each epoch. The

integer ambiguity term is removed from the data series because the baseline is shorter than a full cycle. A bias of less than a cycle remains because of the so-called line bias. This bias can be removed because the multipath error cannot be larger than $\frac{1}{4}$ of a cycle.

What is left in the SD is hereinafter referred to as the residual carrier phase single difference $\Delta\tilde{\Phi}$:

$$\Delta\tilde{\Phi} = \Delta m + \Delta \varepsilon, \quad (3)$$

where Δm and $\Delta \varepsilon$ represent single difference multipath and noise respectively. The residual carrier phase single difference feeds the EKF.

The estimation process requires a minimum of four observations to allow the estimation of the four multipath parameters. Therefore, the estimated multipath parameters represent multipath for the period of time corresponding to four observations. That is why the methodology uses the assumption that multipath has a slow variation over a very short time period.

Following this estimation, other quantities can be derived, such as the multipath at both antennas. These quantities can be subtracted from the original observations yielding multipath-free observations for the reference antenna.

3 Data Collection

GPS data was collected on the roof of Head Hall, on the campus of the University of New Brunswick, throughout June 2000. NovAtel equipment was used: two 501 antennas linked to a single BeeLine GPS receiver. The BeeLine is a 16-channel L1 receiver, in which 8 channels are dedicated to each one of the antennas. The 501 antenna has a diameter of 11 cm. The main reflecting sources are two nearby buildings, 5 m high, distanced from the antennas by 12 m and 18 m; the 1.5 m high parapets at a distance of 4 m and 15 m; and three pillars, all 1.3 m high, located 3 and 6 m away from the antennas. Figure 1 shows the antenna array. Data were collected at 1 and at 0.5-second rates. We are using the 1-second rate data for the analysis shown in this paper.

4 Data Analysis

This paper investigates the multipath parameter estimation process by comparing the spectra of

residual SD time series with the spectra of time series computed from the estimated multipath parameters. These two time series are given by equations (3) and (1), respectively. For this investigation we have used the method of least squares spectral analysis. A description of this method is found in Vaníček [1971], Wells et al. [1985], and Pagiatakis [1999].



Fig 1 The antenna array during data collection.

The data analysis was carried out for several satellites observed in three consecutive days (June 19, 20 and 21). In this paper we are showing results for satellite 26, which are typical from similar analysis to other satellites. This satellite was observed for daily periods of nearly 1.5 hour.

The two data series being analysed have different sizes. The residual SD time series is composed of 5232 entries (one for each observation), whereas the time series of the differential error due to multipath is four times smaller. The latter time series is four times smaller because four observations are needed for the estimation of one set of multipath parameters by the EKF. For the least-squares spectral analysis it is important that the time series span the same time period, which is the case. From the local geometry it is expected that multipath will occur with periods of the order of tens of minutes.

Figures 2, 3 and 4 show the least-squares spectrum of the residual SD (input of the EKF) for days 19, 20 and 21. Figures 5, 6 and 7 show the spectrum of the differential multipath for the same days (computed using the estimated multipath parameters), referred to in the figures as synthetic signal. The vertical axes show the spectral power in terms of percentage of variance, whereas the horizontal axis is divided into units of cycles per

hour (cph). Inside the plots there are indications of the confidence level of the spectral analysis and also inside the boxes are the values, in seconds, of the three most prominent spectral peaks.

The analysis of the figures should be carried out in pairs, referring to the same day: Figures 2 and 5, for day 19, Figures 3 and 6, for day 20, and Figures 4 and 7, for day 21. From the figures a positive correlation between the resulting spectra can be noted. The main peaks, due to multipath, are in the high 30s, mid-20s and mid-10s of seconds. Other small spectral peaks can be seen in the figures but they have no significant meaning for our analysis, some of them being side lobe artifacts. The period corresponding to the noise is left aside in those figures. The peaks correspond to the same period values with some slight differences on days 19 and on 20. Intriguing on day 21 is the peak of 26 minutes, which has not been well explained yet but can be an artifact. The higher confidence level for the spectra of the residual SD time series comes from the fact that it contains more data. The spectral power (given in percentage of variance) of the peaks is slightly different; this can be explained also by the different sizes of both time series.

Figures 8 and 9 show the steadiness of the period estimate for both time series, for the three days. These figures show the same information as in the previous figures but in a different form. It can be seen that the period estimates form a quasi-planar surface, with a small skew on the third day. The planarity reinforces the similarity in the spectral signature of the multipath periods.

The similar spectral signature between the two time series suggests the correctness of the multipath parameters in the estimation process.

5 Concluding Remarks

A methodology aimed at detecting and mitigating static multipath impacting on an array of two closely spaced antennas linked to the same receiver has been presented. One of the antennas, the reference antenna, plays the role of a reference station. In this methodology, multipath parameters are estimated by means of an EKF, which is fed by residual SD carrier phase measurements. This paper shows an assessment of the efficiency of the estimation process. This assessment has been carried out in the spectral domain by comparing the spectra of the residual SD time series with the spectra of time

series of computed differential multipath based upon the estimated multipath parameters. The assessment involves data collected on consecutive days. The decreased confidence level of the differential multipath, in the spectrum, is a consequence of the small dimension of their time series. The spectra of both time series, at the periods in which multipath takes place, are similar, meaning that the estimation process is capable of efficiently retrieving them. This is very important because it allows us to move to another step, which is to generate multipath-mitigated time series by removing the estimated multipath from the original observations.

6 Acknowledgements

We would like to thank Mr. Mensur Omerbashich with his invaluable help processing the least-squares spectral analysis software. The work described in this paper has been supported in part by a grant from the National Sciences and Engineering Research Council of Canada (NSERC).

References

- Axelrad, P., C. Comp and P. K. Macdoran (1994). "Use of signal-to-noise ratio for multipath error correction in GPS differential phase measurements: methodology and experimental results." *Proceedings of the International Technical Meeting of The Institute of Navigation*, Salt Lake City, Utah, July, pp. 655-666.
- Farret, J. C. F. and M. C. Santos (2000). "An alternative method for detection and mitigation of static multipath in L1 carrier phase measurements" *Proceedings of the Institute of Navigation National Technical Meeting*, 22-24 January, Long Beach, Calif., pp. 261-270.
- Hatch, R. (1982). "The synergism of GPS code and carrier measurement." *International Geodetic Symposium on Satellite Doppler Positioning*, Vol. 3, Washington, D.C., pp. 1213-1231.
- Kim, D. and R. B. Langley (1999). "An optimized least-squares technique for improving ambiguity resolution and computational efficiency." *Proceedings of the International Technical Meeting of The Institute of Navigation*, Kansas City, Mo., September, pp. 1579-1588.
- Raquet, J. and G. Lachapelle (1996). "Determination and reduction of GPS reference station multipath using multiple receivers." *Proceedings of the International Technical Meeting of The Institute of Navigation*, Kansas City, Mo., September, pp. 673-681.
- Ray, J. K., M. E. Cannon and P. C. Fenton (1999). "Mitigation of static carrier-phase multipath effects using multiple closely spaced antennas." *Navigation: Journal of the Institute of Navigation*, Vol. 46, No. 3, pp. 193-201.
- Reichert, A. and P. Axelrad (1999). GPS carrier phase multipath reduction using SNR measurements to characterize an effective reflector." *Proceedings of the International Technical Meeting of The Institute of Navigation*, Nashville, Tenn., September, pp. 1951-1960.
- Pagiatakis, S. D. (1999). "Stochastic significance of peaks in the least-squares spectrum." *Journal of Geodesy*, Vol. 75, pp. 67-78.
- Vaníček, P. (1971). "Further developments and properties of the Least Squares Spectral Analysis." *Astrophysics and Space Science*, Vol. 12, pp. 357-367.
- Wells, D., P. Vaníček and S. D. Pagiatakis (1985). "Least squares spectral analysis revisited." Department of Geodesy and Geomatics Engineering Technical Report No. 84, University of New Brunswick, Fredericton, NB, Canada
- Wells, D., N. Beck, D. Delikaraoglou, A. Kleusberg, E. J. Krakiwsky, G. Lachapelle, R. B. Langley, M. Nakiboglu, K. P. Schwarz, J. M. Tranquilla, and P. Vaníček (1986). *Guide to GPS Positioning*, Canadian GPS Associates.

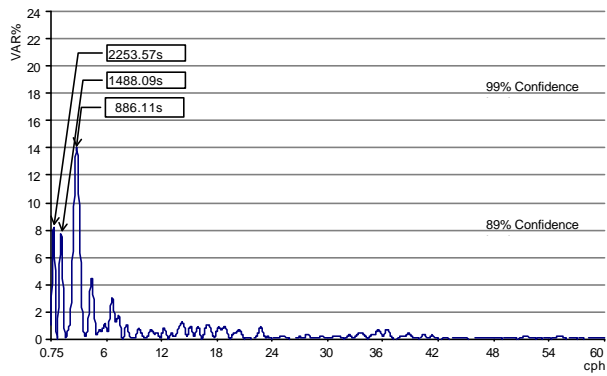


Fig 2 Least-squares spectrum of residual SD, periods between 1min and $\frac{3}{4}$ hrs, day 19.

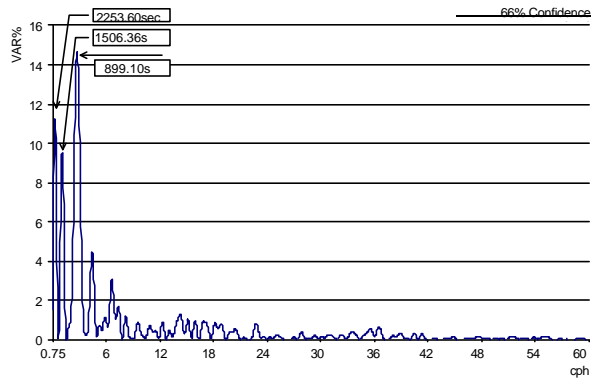


Fig 5 Least-squares spectrum of synthetic signal, periods between 1min and $\frac{3}{4}$ hrs, day 19.

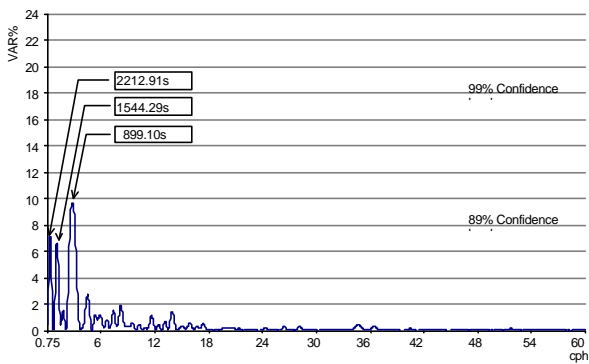


Fig 3 Least-squares spectrum of residual SD, periods between 1min and $\frac{3}{4}$ hrs, day 20.

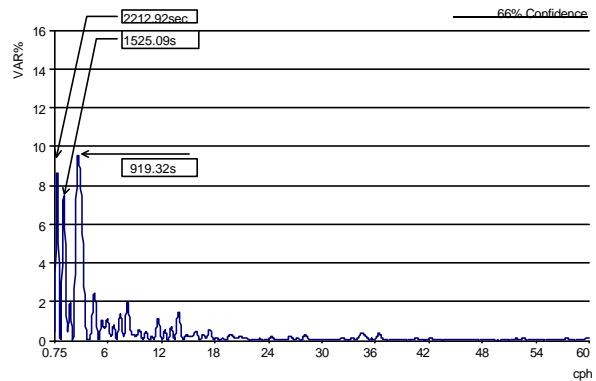


Fig 6 Least-squares spectrum of synthetic signal, periods between 1min and $\frac{3}{4}$ hrs, day 20.

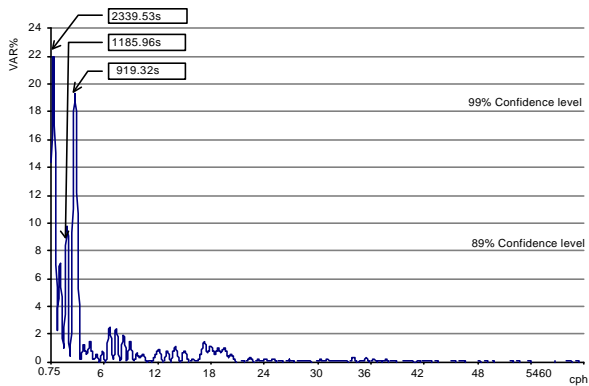


Fig 4 Least-squares spectrum of residual SD, periods between 1min and $\frac{3}{4}$ hrs, day 21.

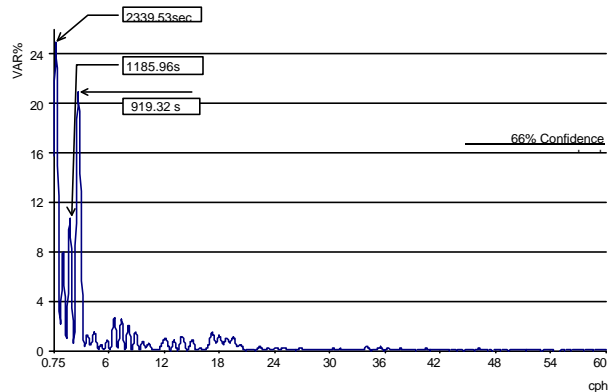


Fig 7 Least-squares spectrum of synthetic signal, periods between 1min and $\frac{3}{4}$ hrs, day 21.

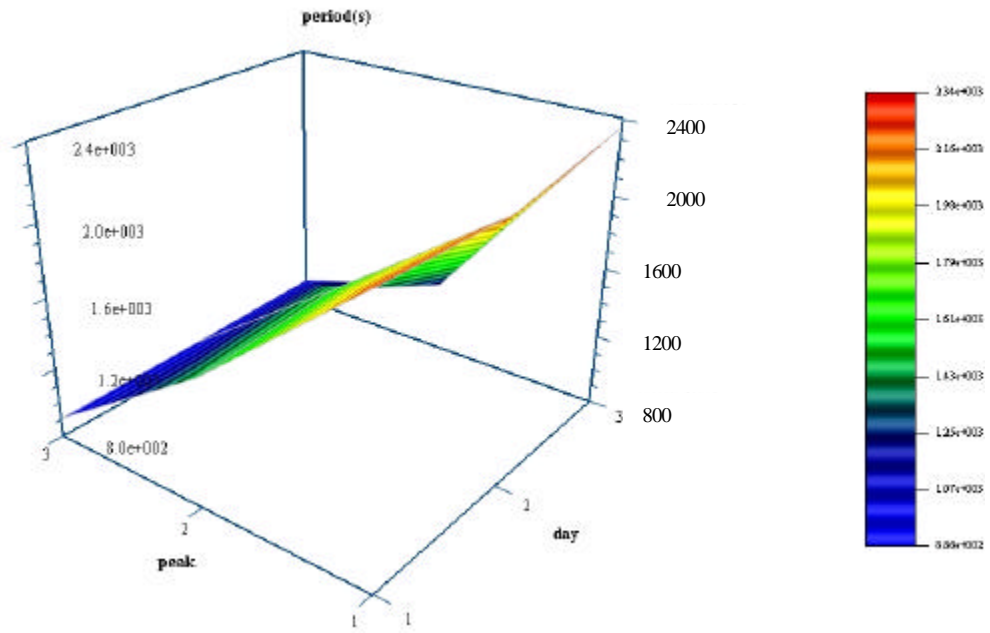


Fig 8 Steadiness of spectral period estimates for the three days (from residual single difference).

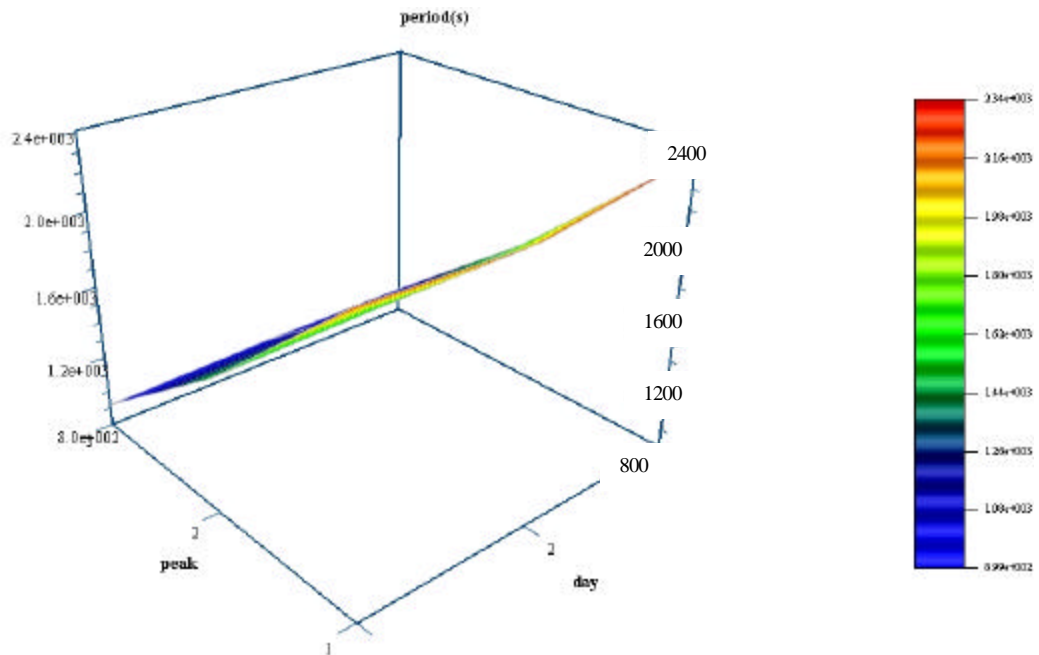


Fig 9 Steadiness of spectral period estimates for the three days (from synthetic signal).